

The following resources related to this article are available online at www.sciencemag.org (this information is current as of December 4, 2009):

Updated information and services, including high-resolution figures, can be found in the online version of this article at:

<http://www.sciencemag.org/cgi/content/full/282/5397/2241>

This article **cites 20 articles**, 8 of which can be accessed for free:

<http://www.sciencemag.org/cgi/content/full/282/5397/2241#otherarticles>

This article has been **cited by** 47 article(s) on the ISI Web of Science.

This article has been **cited by** 13 articles hosted by HighWire Press; see:

<http://www.sciencemag.org/cgi/content/full/282/5397/2241#otherarticles>

This article appears in the following **subject collections**:

Geochemistry, Geophysics

http://www.sciencemag.org/cgi/collection/geochem_phys

Information about obtaining **reprints** of this article or about obtaining **permission to reproduce this article** in whole or in part can be found at:

<http://www.sciencemag.org/about/permissions.dtl>

- powder is given by $p_c = [1 + \xi \phi / (4 x_c)]^{-1}$, where ϕ is a reciprocal planar packing factor, and x_c is a critical surface area fraction of the larger particles, which must be covered for percolation by the smaller particles. Values based on microstructural analysis giving good agreement with conductivity experiments are $x_c = 0.42$ and $\phi = 1.27$, which we have also used as a reasonable approximation for sea ice.
24. J. T. Chayes and L. Chayes, *Commun. Math. Phys.* **105**, 133 (1986).
25. M. G. McPhee *et al.*, *Bull. Am. Meteorol. Soc.* **77**, 1221 (1996).
26. S. F. Ackley, V. I. Lytle, K. M. Golden, M. N. Darling, G. A. Kuehn, *Antarctic J. U.S.* **30**, 133 (1995).
27. V. I. Lytle, R. Massom, N. Bindoff, A. P. Worby, I. Allison, *J. Geophys. Res.*, in press.
28. K. M. Golden, *Phys. Rev. Lett.* **78**, 3935 (1997).
29. S. A. Arcone, A. J. Gow, S. McGrew, *J. Geophys. Res.* **91**, 14281 (1986).
30. We thank the participants of the ANZFLUX and HIHO HIHO experiments and the crews of the *R.V.*

Nathaniel B. Palmer and the *R.S.V. Aurora Australis* for contributing to the field work yielding the data we report. We also thank M. McPhee, D. Perovich, H. Eicken, and A. Efors for helpful discussions and P. Heil, A. Worby, and two anonymous reviewers for helpful comments on the manuscript. Supported by NSF grants OPP-97-25038, DMS-96-22367, and Office of Naval Research grant N00014-93-10141 to K.M.G. and NSF grant OPP-93-15934 to S.F.A.

16 September 1998; accepted 10 November 1998

Evidence for Extreme Climatic Warmth from Late Cretaceous Arctic Vertebrates

J. A. Tarduno,* D. B. Brinkman, P. R. Renne, R. D. Cottrell, H. Scher, P. Castillo

A Late Cretaceous (92 to 86 million years ago) vertebrate assemblage from the high Canadian Arctic (Axel Heiberg Island) implies that polar climates were warm (mean annual temperature exceeding 14°C) rather than near freezing. The assemblage includes large (2.4 meters long) champsosaurs, which are extinct crocodilelike reptiles. Magmatism at six large igneous provinces at this time suggests that volcanic carbon dioxide emissions helped cause the global warmth.

The Cretaceous is commonly considered to have been ice-free with high atmospheric CO₂ levels (1–3), but some isotopic and paleofloral evidence has implied that polar temperatures were near freezing (4–6). Here we describe a fossil vertebrate assemblage from the high Canadian Arctic that supports a Late Cretaceous [92 to 86 million years ago (Ma)] thermal maximum.

The Cretaceous of the Canadian Arctic is represented by sedimentary and volcanic rocks of the Sverdrup Basin (7), which are exceptionally well exposed on western Axel Heiberg Island (Fig. 1). The youngest rocks in the area are Late Cretaceous to Eocene sedimentary rocks of the Eureka Sound Group. Shallow marine to continental shale, siltstone, and sandstone are underlain by Late Cretaceous marine shale of the Kanguk Formation. On much of western Axel Heiberg Island, the Kanguk Formation unconformably overlies subaerially erupted flood basalts of the Cretaceous Strand Fiord Formation. These lavas are part of a large magmatic pulse, or large igneous province, that may include large parts of Ellesmere Island and

the Arctic Ocean basin (8).

Near Expedition Fiord (79°23.5'N, 92°10.9'W), sedimentary rocks record the transition between the Strand Fiord lavas and Kanguk shale. The uppermost flow of the Strand Fiord Formation is overlain by 0.6 m of weathered basalt and soil (Fig. 1). The soil is overlain by approximately 3.0 m of shale and siltstone, which may represent a bay or estuary. We found well-preserved vertebrate fossils in several of the thin siltstone horizons in this sequence. Although disarticulated, related bones were in close proximity, suggesting limited transport.

Recent magnetostratigraphic study (9) at Strand Fiord (Fig. 1) suggests that the base of the Kanguk Formation is older than 83.5 Ma (geomagnetic chron 33R) (10). Ammonites of the *Scaphites depressus* Zone indicate that the Kanguk Formation 194 m above its base at Glacier Fiord (11) is of late Coniacian age (~86.0 to 87.0 Ma). Ammonites suggest that the basal Kanguk Formation is late early Turonian in age (~92.0 to 91.0 Ma) on Amund Ringes Island (7). ⁴⁰Ar/³⁹Ar incremental heating (12) of a whole-rock sample from the upper lava flows at Strand Fiord (9) has yielded an 11-step plateau (Fig. 2). These data indicate an age of 95.3 ± 0.2 Ma near the Cenomanian-Turonian boundary (13). U/Pb zircon analyses of gabbroic intrusions on northwestern Ellesmere Island, thought to be part of the same magmatic event as that represented by the Strand Fiord Formation, yield an age of 92.0 ± 1.0 Ma (early Turonian) (14). Together these data indicate that the vertebrate fossil

assemblage is Turonian to Coniacian (~92 to 86 Ma) in age.

The fossils represent a diverse assemblage of nonmarine aquatic and semiaquatic vertebrates (Fig. 3), including fish, turtles, and champsosaurs. At least two types of fish are represented by scales similar to those described as Holostean A and Holostean B from Upper Cretaceous nonmarine sediments (15). Turtles and champsosaurs offer several advantages over other fossils used as climatic indicators, such as the latest Cretaceous dinosaurs of the North Slope, Alaska, because they are free from ambiguities posed by possible migration and warm-bloodedness (16, 17). Turtles are represented by costals and peripherals that are comparable to shell elements of generalized aquatic cryptodires. Extant aquatic nonmarine turtles are ectothermic reptiles and have a climatically limited distribution. The length and warmth of summers limit turtle distributions, primarily by affecting the survival of eggs and hatchlings. The cold-adapted turtles *Chelydra serpentina* and *Chrysemys picta* provide a conservative estimate of the growing season required (18). Viable populations of these taxa are restricted to areas where the growing season has at least 100 frost-free days per year (19).

Maximum temperatures during the warmest month of the year also provide a measure of the climatic requirements of these cold-adapted turtles. Naturally occurring viable populations of *Chelydra serpentina* and *Chrysemys picta* do not occur in areas with a warm-month average maximum temperature of less than 25°C (18, 19). This measure corresponds to a warm-month mean temperature of 17.5°C and a mean annual temperature of 2.5°C. Thus, by analogy, the turtles in the Late Cretaceous Axel Heiberg locality indicate that the mean annual temperature was at least 2°C, the warm-month average maximum temperature was at least 25°C, and the climate was frost-free for more than 100 days per year.

The Axel Heiberg vertebrate assemblage differs from others known from the Upper Cretaceous of Arctic North America in the abundance of semiaquatic reptiles (20) and in the presence of champsosaurs. Champsosaurs, which are thought to have been active semiaquatic predators (21), are represented by a tibia, a mandible, an ulna, femurs, ribs, gastralia, ischia, and centra (Fig. 3). The mandible fragment indicates that the snout was long and

J. A. Tarduno, R. D. Cottrell, H. Scher, Department of Earth and Environmental Sciences, University of Rochester, Rochester, NY, 14627, USA. D. B. Brinkman, Royal Tyrrell Museum of Palaeontology, Drumheller, Alberta, TOJ OYO, Canada. P. R. Renne, Berkeley Geochronology Center, Berkeley, CA 94709, USA. P. Castillo, Geological Research Division, Scripps Institution of Oceanography, La Jolla, CA 92093-0220, USA.

*To whom correspondence should be addressed. E-mail: john@earth.rochester.edu

slender, comparable to that of the genus *Champsosaurus* from Upper Cretaceous and Paleocene rocks at lower latitudes elsewhere in North America. A substantial size range was present. A complete tibia allows us to estimate the length of one of the larger individuals by comparison with published data (22) and a similarly sized specimen in the collection of the Royal Tyrrell Museum of Paleontology (specimen RTMP 86.12.11). On the basis of this element, the length of champsosaurs from the Arctic locality reached at least 2.4 m.

As in extant ectothermic reptiles, temperature would have been a primary control on the distribution of champsosaurs. Tolerances can be hypothesized from the temperature limits of the extant reptiles that phylogenetically bracket champsosaurs. Recent analyses place champsosaurs in a primitive position in the Archosauromorpha (23), so the group is bracketed by crocodylians and lepidosauromorphs among living reptiles; the closest living relatives are crocodiles. Crocodiles are also the closest modern analogs in terms of body proportions, size, and mode of life. The thermal limit for viable populations of crocodiles is marked by a coldest-month mean temperature (24) of $\sim 5.5^\circ\text{C}$. The preferred operating temperature of crocodiles is 25° to 35°C , and this temperature is maintained for sufficient duration in areas with a minimum mean annual temperature greater than 14°C .

In lepidosauromorphs, the ability to tolerate climate extremes is size-related. Large lepidosaurs are unable to escape subcritical temperatures by behavioral or physiological means (24). Extant lepidosauromorphs with a body size comparable to the Arctic champsosaurs reported here, such as varanids and large iguanids, are more restricted in their temperature tolerances than are crocodiles. Thus, based on tolerances in the extant reptiles that phylogenetically bracket champsosaurs and are comparable in size, the most conservative estimate of the temperature tolerance of champsosaurs is provided by crocodylians, and these suggest that the mean annual temperature in this region was greater than 14°C . An inherent uncertainty is associated with this temperature estimate because champsosaurs are extinct. The discrepancy between the climate implied by the overall fossil assemblage and one where freezing conditions would be common is nevertheless large.

On the basis of global paleomagnetic data (25), our new fossil locality was at a paleolatitude of $72^\circ \pm 4^\circ\text{N}$ (Fig. 1). Potential tectonic motions within the Canadian Arctic allow for slightly lower or higher values (26) beyond the 95% confidence interval quoted. However, a paleolatitude above the Late Cretaceous Arctic circle appears most likely for our site.

Turonian fossil flora from Kamchatka (3) (paleolatitude $\sim 70^\circ$) (25) suggest that the mean annual temperature was at least 7°C there and that the cold-month mean temperature was -4°C . Turonian flora from Novaya

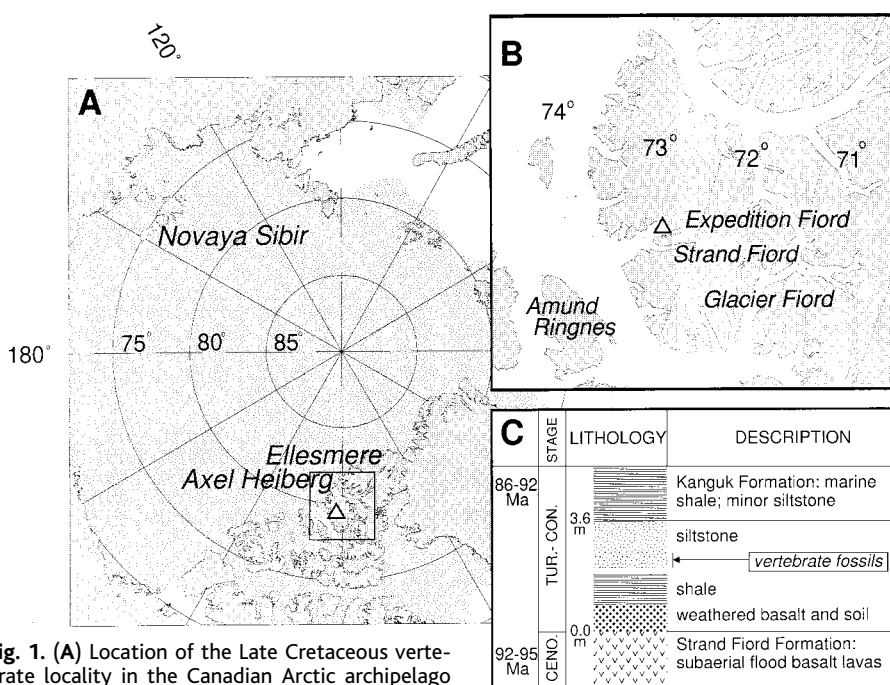


Fig. 1. (A) Location of the Late Cretaceous vertebrate locality in the Canadian Arctic archipelago (triangle). Sea ice is shown in a stippled pattern. (B) Paleolatitude lines (dashed) using 90-Ma pole for North America (25). (C) Stratigraphic column showing vertebrate-bearing sedimentary layers from Expedition Fiord. Numerical ages for the basal Kanguk Formation are based on published time scales (10). The age for Cretaceous Arctic magmatism is based on new $^{40}\text{Ar}/^{39}\text{Ar}$ radiometric age data from the Strand Fiord Formation (this work) and Pb/U radiometric age data from gabbroic intrusions on Ellesmere Island (14).

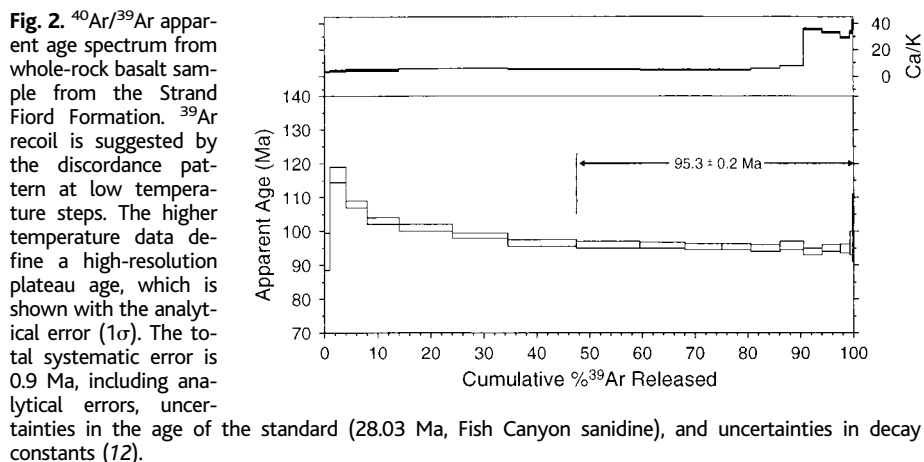


Fig. 2. $^{40}\text{Ar}/^{39}\text{Ar}$ apparent age spectrum from whole-rock basalt sample from the Strand Fiord Formation. ^{39}Ar recoil is suggested by the discordance pattern at low temperature steps. The higher temperature data define a high-resolution plateau age, which is shown with the analytical error (1σ). The total systematic error is 0.9 Ma, including analytical errors, uncertainties in the age of the standard (28.03 Ma, Fish Canyon sanidine), and uncertainties in decay constants (12).

Sibir (3) (Fig. 1) in the Russian Arctic (paleolatitude $\sim 78^\circ$) (25) yield a mean annual temperature of 9°C and a cold-month mean temperature of 0°C . Because of the lowered metabolic and reproductive rates, it is doubtful that viable populations of large-bodied, active, ectothermic reptiles could be maintained under the seasonal freezing conditions implied by these monthly average temperature estimates. The fossil floral sites are adjacent to oceans, so the discrepancy between these cooler estimates and those implied by the Axel Heiberg fossil reptiles cannot be due to a continental climate gradient. Determining whether the difference reflects distance from a source of warm water currents, such as the

Western Interior Seaway (3), must await results from additional sites. A similar discrepancy between temperature estimates based on flora and vertebrates has been noted for the early Cenozoic (27). However, the differences might reflect age differences [1 to 2 million years (My)] between the new Arctic vertebrate data and the fossil flora sites.

An increased flux of volcanic CO_2 has often been offered as a mechanism for driving Cretaceous greenhouse warming, but only recently has a detailed temporal picture of volcanism become available. In addition to volcanism in the Arctic, basaltic volcanism occurred at five large igneous provinces during Turonian-Cenozoic times, including (Fig. 4) emplace-

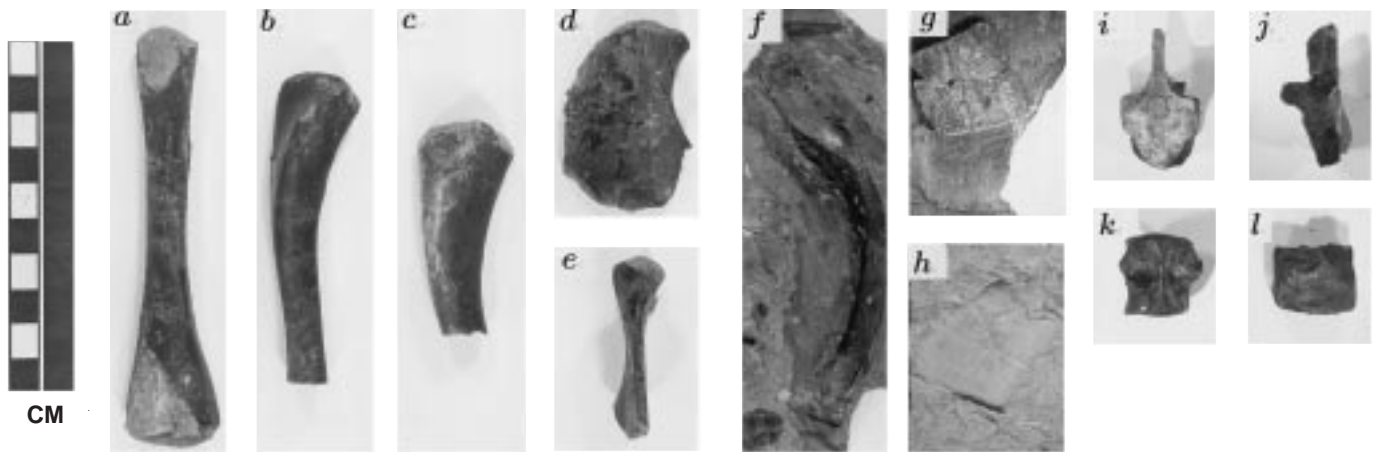


Fig. 3. Late Cretaceous vertebrate fossils from Axel Heiberg Island. (A) through (F) are from champsosaurs. (A) Tibia; (B and C) femurs; (D) ischium; (E) same as (D), side view; (F) rib; (G) turtle peripheral bones; (H) turtle peripheral showing sulci; (I) champsosaur dorsal centrum; (J) same as (I), side view; (K) champsosaur second cervical centrum; (L) same as (K), side view.

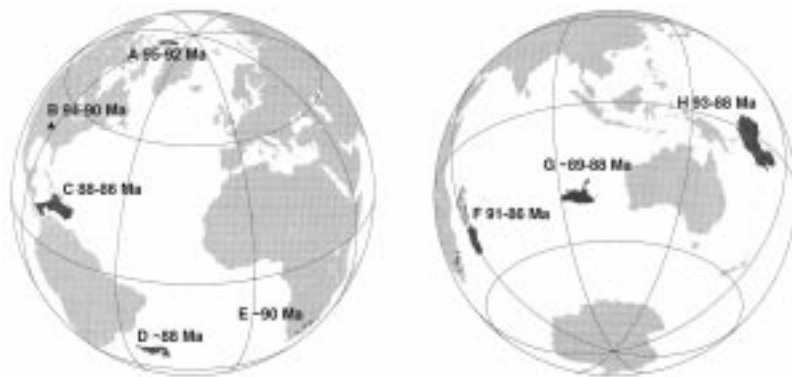


Fig. 4. Late Cretaceous large igneous provinces, kimberlites, and alkalic intrusions. (A) High Arctic large igneous province (8) (this paper). (B) North American alkalic intrusions (34). (C) Caribbean Oceanic Plateau (28). (D) Rio Grande Rise (31). (E) South African Group II kimberlites (33). (F) Madagascar flood basalts and possibly coeval oceanic flood basalts (29). (G) Broken Ridge (30). (H) Late Cretaceous Ontong Java Plateau volcanism (32).

ment of the Caribbean Oceanic Plateau (28), eruption of the Madagascar flood basalts (29), volcanism at Broken Ridge (30), emplacement of large parts of the Rio Grande Rise (31), and renewed volcanism on the Ontong Java Plateau (32). The Late Cretaceous also saw the emplacement of kimberlites in South Africa (33) and of alkalic rocks in the southern United States (34). Together these events define a restricted interval (<7 My) of extraordinary global magmatism. If the short-term (1000- to 100,000-year) effusion rates at these large igneous provinces were many times those averaged over several million years (35), CO₂ input to the atmosphere could have stimulated greenhouse conditions and the warmth implied at our Arctic site.

The presence of reptiles at Arctic latitudes offers challenges for efforts to model Cretaceous climates. The high polar temperatures implied here exacerbate the problems of simulating warm polar conditions without also raising equatorial temperatures to unreasonably high values (36). The

warm equable climate that is often associated with the Cretaceous probably did not characterize the entire period (17). Some data suggest relatively cool climates in the Early Cretaceous (37). Nevertheless, the Arctic vertebrates and coeval global volcanism suggest that the Greenhouse Earth analog (1) may be found in the Turonian-Coniacian time interval.

References and Notes

1. T. J. Crowley and K.-Y. Kim, *Geophys. Res. Lett.* **22**, 933 (1995).
2. B. T. Huber, D. A. Hodell, C. P. Hamilton, *Geol. Soc. Am. Bull.* **107**, 1164 (1995).
3. A. B. Herman and R. A. Spicer, *Nature* **380**, 330 (1996).
4. B. W. Sellwood, G. D. Price, P. J. Valdes, *ibid.* **370**, 453 (1994).
5. G. D. Price, B. W. Sellwood, D. Pirrie, *Geol. Soc. Am. Bull.* **108**, 1192 (1996).
6. R. A. Spicer and J. T. Parrish, *J. Geol. Soc. London* **147**, 329 (1990).
7. H. R. Balkwill, *Am. Assoc. Petrol. Geol. Bull.* **62**, 1004 (1978).
8. J. A. Tarduno, *Suppl. Trans. Am. Geophys. Union* **77**, 844 (1996).

9. J. A. Tarduno, R. D. Cottrell, S. L. Wilkison, *J. Geophys. Res.* **102**, 723 (1997).
10. F. M. Gradstein *et al.*, *ibid.* **99**, 24051 (1994).
11. L. V. Hills, W. F. Braunerger, L. K. Nunezbetelu, R. L. Hall, *Can. J. Earth Sci.* **31**, 733 (1994).
12. P. R. Renne *et al.*, *Chem. Geol.* **149**, 259 (1998).
13. B. J. Kowallis, E. H. Christiansen, A. L. Deino, M. J. Kunk, L. M. Heaman, *Cretaceous Res.* **16**, 109 (1995).
14. H. P. Trettin and R. Parrish, *Can. J. Earth Sci.* **24**, 257 (1987).
15. D. B. Brinkman, *Palaeogeogr. Palaeoclimatol. Palaeoecol.* **78**, 37 (1990).
16. J. M. Parrish, J. T. Parrish, J. H. Hutchison, R. A. Spicer, *Palaios* **2**, 377 (1987).
17. The striking absence of champsosaurs and crocodyles in polar vertebrate assemblages containing dinosaurs could indicate that some stages of the Cretaceous were cooler than the Turonian-Coniacian interval.
18. J. B. Iverson, "A revised checklist with distribution maps of the turtles of the world" (Earlham College, Richmond, IN, 1992).
19. *The National Atlas of Canada* (Macmillan, Toronto, Canada, 1974).
20. A turtle is known from the Cenomanian North Slope of Alaska, but no champsosaur material is known from this area. Hadrosaur material was collected from the latest Cretaceous of Bylot Island and Alaska, but no freshwater reptile material was recovered at either locality.
21. B. R. Erickson, *Sci. Mus. Minn. Monogr. Paleontol.* **1**, 1 (1972).
22. B. R. Erickson, *J. Verteb. Paleontol.* **5**, 111 (1985).
23. S. Evans, *Zool. J. Linn. Soc.* **90**, 205 (1990).
24. P. J. Markwick, *Palaeogeogr. Palaeoclimatol. Palaeoecol.* **137**, 205 (1998).
25. J. Besse and V. Courtillot, *J. Geophys. Res.* **96**, 4029 (1991).
26. P. J. Wynne, E. Irving, K. G. Osadetz, *Can. J. Earth Sci.* **25**, 1220 (1988).
27. J. H. Hutchison, *Palaeogeogr. Palaeoclimatol. Palaeoecol.* **37**, 149 (1982).
28. A. C. Kerr *et al.*, *Lithos* **37**, 245 (1996).
29. M. Storey *et al.*, *Science* **267**, 852 (1995).
30. R. A. Duncan, *Proc. Ocean Drill. Prog. Sci. Res.* **121**, 507 (1991).
31. J. M. O'Connor and R. A. Duncan, *J. Geophys. Res.* **95**, 17475 (1990).
32. M. L. G. Tejada, J. J. Mahoney, R. A. Duncan, M. P. Hawkins, *J. Petrol.* **37**, 361 (1996).
33. R. B. Hargraves, *J. Geophys. Res.* **94**, 1851 (1989).
34. A. K. Baksi, *J. Geol.* **105**, 629 (1997).
35. J. C. Varekamp, R. Keulen, R. R. E. Porter, M. J. Van Bergen, *Terra Nova* **4**, 363 (1992).
36. E. J. Barron and W. M. Washington, in *The Carbon Cycle and Atmospheric CO₂: Natural Variations Archean to Present*, E. T. Sundquist and W. S. Broecker, Eds. [Geo-

- phys. Monogr. Am. Geophys. Union* 32 (1985)], p. 546.
 37. H. M. Stoll and D. P. Schrag, *Science* 272, 1771 (1996).
 38. We thank the Canadian Polar Continental Shelf Project for their invaluable field support; R. Lundgren, O. Libman, J. Totten, and K. Weaver for help in the field; G.

Kloc, S. Wilkison, and S. Pruss for assistance in sample preparations; and J. Massare and D. Woodrow for helpful discussions. Supported by the U.S. NSF Arctic Natural Sciences Division.

21 September 1998; accepted 10 November 1998

Hierarchically Ordered Oxides

Peidong Yang, Tao Deng, Dongyuan Zhao, Pingyun Feng, David Pine, Bradley F. Chmelka, George M. Whitesides, Galen D. Stucky*

Porous silica, niobia, and titania with three-dimensional structures patterned over multiple length scales were prepared by combining micromolding, polystyrene sphere templating, and cooperative assembly of inorganic sol-gel species with amphiphilic triblock copolymers. The resulting materials show hierarchical ordering over several discrete and tunable length scales ranging from 10 nanometers to several micrometers. The respective ordered structures can be independently modified by choosing different mold patterns, latex spheres, and block copolymers. The examples presented demonstrate the compositional and structural diversities that are possible with this simple approach.

Several approaches are currently available for the preparation of ordered structures at different length scales. For example, organic molecular templates can be used to form crystalline zeolite-type structures with ordering lengths less than 3 nm (1); mesoporous materials with ordering lengths of 3 to 30 nm can be obtained using surfactants or amphiphilic block copolymers as structure-directing agents (2–7); the use of latex spheres yields macroporous materials with ordering lengths of 100 nm to 1 μm (8–13); and soft lithography can be used to make high-quality patterns and structures with lateral dimensions of about 30 nm to 500 μm (14–16). Despite all of these efforts in nanostructuring materials, the fabrication of hierarchically ordered structures at multiple length scales, such as seen in nature in diatoms (17), has remained an experimental challenge. Such materials are important both for the systematic fundamental study of structure-property relations and for their technological promise in applications such as catalysis, selective separations, sensor arrays, wave guides, miniaturized electronic and magnetic devices, and photonic crystals with tunable band gaps.

Previously, micromolding has been used to form patterned mesoporous materials (18, 19). These studies, however, used acidic aqueous conditions to carry out the cooperative self-assembly (20), which is disadvantageous because

of the limited processibility of the aqueous solutions. Either noncontinuous films were formed (18) or an electric field was needed to guide pattern formation, which requires a nonconducting substrate (19). Latex spheres have also been used to make disordered macro- and mesoporous silica (9). We have developed a simple procedure for preparing hierarchically ordered structures by concurrently or sequentially combining micromolding, latex sphere templating, and cooperative assembly of hydrolyzed inorganic species (metal alkoxides, metal chlorides) and amphiphilic block copolymers. The materials generated from this process exhibit structural ordering at multiple discrete length scales (in this case, 10, 100, and 1000 nm). Patterned macro- and meso-

porous materials of various compositions, including silica, niobia, and titania, were synthesized. Such multiple-scale structural organization makes it possible to tune the physical properties of the materials over a wide range of chemical compositions.

The scheme in Fig. 1A illustrates the procedure that was used to fabricate materials with two-scale ordering. Gelation of a self-assembling sol-gel precursor solution was carried out in the confined space of a poly(dimethylsiloxane) (PDMS) mold (14). The precursor solution has the same composition as used in the preparation of mesoporous silica films (3, 21)—that is, expressed as molar ratios, 0.008 to 0.018 poly(ethyleneoxide)-*b*-poly(propyleneoxide)-*b*-poly(ethyleneoxide) (EO_{*n*}PO_{*m*}EO_{*n*}); 1 tetraethoxysilane (TEOS); 20 to 60 ethanol (EtOH); 0.01 to 0.04 HCl; and 5 to 10 H₂O. When Pluronic F127 (EO₁₀₆PO₇₀EO₁₀₆) was used as the structure-directing block copolymer species, a cubic mesophase resulted, whereas a hexagonal mesophase was obtained when Pluronic P123 (EO₂₀PO₇₀EO₂₀) was used (21). This sol-gel mesophase chemistry has recently been extended to the preparation of diverse thermally stable mesostructured transition metal oxides, including Nb₂O₅, TiO₂, ZrO₂, WO₃, AlSiO_{3.5}, and SiTiO₄, by slowing the hydrolysis of inorganic chloride precursor species in alcohol solutions (4). These materials were molded by placing a drop of the precursor solution on a freshly cleaned substrate (such as a silicon wafer), after which the mold was placed face down to cover the drop on the surface of the substrate. A pressure of roughly 1 × 10⁵ to 2 × 10⁵ Pa was applied to the PDMS mold. The area of the patterned surface was typically 1 to 5 cm², with molded feature sizes in

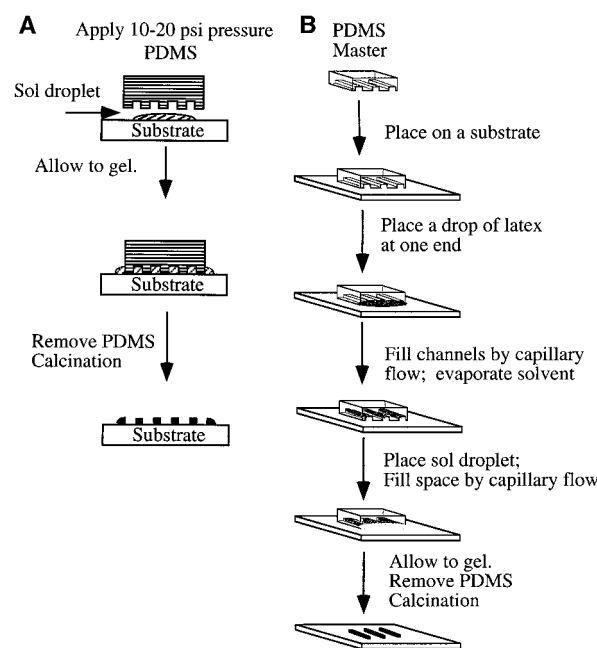


Fig. 1. Schematic diagrams of the molding methods used to fabricate hierarchically ordered structures on a substrate. (A) For patterning of mesoporous solids, a droplet of sol-gel-block copolymer precursor solution was compressed between the silicone mold and the substrate by applying a pressure of roughly 1 × 10⁵ to 2 × 10⁵ Pa. The high interfacial free energy of the solution caused the precursor to dewet the substrate where the mold and the substrate were in contact. (B) A sequential process for producing hierarchical ordering over three discrete and independent length scales.

P. Yang, D. Zhao, G. D. Stucky, Department of Chemistry, University of California, Santa Barbara, CA 93106, USA. T. Deng and G. M. Whitesides, Department of Chemistry and Chemical Biology, Harvard University, Cambridge, MA 02138, USA. P. Feng, D. Pine, B. F. Chmelka, Department of Chemical Engineering, University of California, Santa Barbara, CA 93106, USA.

*To whom correspondence should be addressed.